HHS Public Access

Author manuscript

Nat Neurosci. Author manuscript; available in PMC 2015 April 01.

Published in final edited form as:

Nat Neurosci. 2014 October ; 17(10): 1316–1318. doi:10.1038/nn.3806.

Neural compensation in older people with brain β-amyloid deposition

Jeremy A. Elman[1,*,†], **Hwamee Oh**[2,†], **Cindee M. Madison**[2], **Suzanne L. Baker**[1], **Jacob W. Vogel**[2], **Shawn M. Marks**[2], **Sam Crowley**[2], **James P. O'Neil**[1], and **William J. Jagust**[1,2]

[1]Life Sciences Division, Lawrence Berkeley National Laboratory, Berkeley, CA 94720, USA

[2]Helen Wills Neuroscience Institute, University of California, Berkeley, CA 94720, USA

Abstract

The recruitment of additional neural resources may allow elderly adults to maintain normal cognition despite β-amyloid (Aβ) plaques. Previous fMRI studies have reported such hyperactivation, but it is currently unclear if these increases represent compensation or aberrant over-excitation. We found that older adults with Aβ deposition had reduced deactivations in task negative regions, but increased activation in task positive regions related to more detailed memory encoding. The association between higher activity levels and more detailed memories suggests that Aβ-related hyperactivation is a compensatory mechanism, potentially reflecting brain plasticity in response to Aβ deposition.

Many people experience declining episodic memory ability with advancing age, a symptom that is also common in the early stages of Alzheimer's disease (AD). Although the cause of AD is unknown, current theories implicate brain accumulation of the β-amyloid protein (Aβ) as a very early event in AD pathogenesis[1]. Many older people who maintain normal cognitive function have been found at subsequent autopsy to harbor extensive Aβ plaque pathology, and more recent studies using PET imaging agents that bind to Aβ plaques have confirmed this observation *in vivo*[2–4]. The combination of declining memory and Aβ plaque deposits in normal older people suggests that these individuals may be in a preclinical phase of AD[5].

How do some older individuals maintain normal cognition in the face of Aβ deposition, while others succumb to cognitive decline and dementia? Functional magnetic resonance imaging (fMRI) studies of cognitively normal older people with brain Aβ deposition[6,7] and

*Correspondence to: jelman@berkeley.edu.
†Authors contributed equally to this work.

Supplementary Material is linked to the online version of the paper at www.nature.com/neuro.

Author Contributions: J.A.E., H.O., W.J.J. designed the study; J.P.O. synthesized the [^{11}C]PIB; J.W.V. performed neuropsychological testing; S.C. performed PET acquisition; J.A.E. and H.O. performed MRI acquisition; S.L.B., C.M.M. and S.M.M. processed PET data; J.A.E., H.O. and C.M.M. processed MRI data; J.A.E. and H.O. analyzed data; J.A.E., H.O. and W.J.J. prepared the manuscript. J.A.E. and H.O. contributed equally to the study. All authors discussed results and commented on the manuscript.

Author Information: The authors report no competing interests.

those with mild cognitive impairment (MCI)[8] have reported increased neural activity during cognitive activity in comparison to young people or older people without Aβ. However, the question of whether these Aβ-related increases are beneficial or harmful remains unresolved. We sought to address this question by adopting an fMRI task that probed the richness of each encoded stimulus by evaluating how the amount of memory detail was related to the extent of fMRI activation[9].

We studied 22 healthy young subjects, 33 cognitively normal older people with no evidence of brain Aβ (PIB–), and 16 cognitively normal older people with brain Aβ deposition (PIB+) revealed by PET imaging with the amyloid imaging agent [^{11}C]PIB (see Table 1 and Supplementary Table 1 for full subject characteristics). During the acquisition of fMRI data, subjects studied pictures of scenes and were told that they would later be asked questions about these stimuli (Supplementary Fig. 1a). Approximately 15 minutes after scanning, subjects were first tested for their memory of the central meaning of the stimuli ("gist memory"). Subjects viewed a set of written descriptions of scenes and were asked whether each corresponded to a previously studied picture or not (Supplementary Fig. 1b). Following this phase, subjects were required to respond whether each of 6 written details associated with each studied scene was true or false, giving a measure of memory richness (Supplementary Fig. 1c). The fMRI analyses assessed brain activations during encoding for items subsequently remembered during the gist task (hits) compared to baseline, as well as linear increases or decreases in activity related to the number of details remembered. In order to distinguish relative increases and decreases from baseline, we masked the results of these comparisons with task-positive and task-negative network maps derived from comparing hits to baseline averaged across all groups (i.e., Fig. 1a).

All groups performed significantly above chance on both gist and details tasks with no between group differences (Table 1). While young subjects scored better on multiple neuropsychological tests compared to the older groups, there were no differences between the PIB+ and PIB– groups (see Supplementary Table 1). Across all participants, brain regions that were more active during encoding for gist hits resembled the previously described task positive network[10], while areas that were deactivated included large regions of a task negative network commonly referred to as the default mode network (DMN)[11] (Fig. 1a, Supplementary Table 3). Brain regions that showed a parametric increase of activity related to the number of details recalled across groups were largely a subset of the regions activated during gist encoding, while areas exhibiting parametric decreases comprised a subset of the DMN (Fig. 1b, Supplementary Table 4). Brain Aβ in old PIB+ individuals was characteristically deposited throughout medial and lateral association cortex as well as medial frontal cortex (Fig. 1c).

While the primary focus of this study was to assess parametric changes in activity related to memory strength, results of the gist task were broadly consistent with previous findings. Both young and PIB+ individuals demonstrated greater activation for hits compared to baseline within task positive regions compared to PIB– subjects (see Supplementary Fig. 2 and Supplementary Table 5). In contrast, both groups demonstrated reduced deactivations for hits in task negative regions. It should be noted that when hits were compared to misses,

greater relative deactivations occurred in task negative regions for young subjects (Supplementary Fig. 3).

To assess parametric effects, we compared linear increases and decreases of activity across the number of details correctly identified for items remembered on the gist task between groups. The test of age effects compared young and older PIB– subjects, controlling for performance (Gist hit rate), and voxelwise GM volume. Young subjects showed greater detail-related parametric increases than old PIB– subjects throughout lateral and ventral occipital cortex, superior and medial parietal cortex, and inferior temporal cortex (Fig. 2a, Supplementary Table 6). Examining these contrasts using the task-positive and task-negative masks from all participants revealed that most of these differences were due to greater increases in activity with more details remembered within task positive areas in young subjects (Fig. 2b). While old PIB– individuals demonstrated relatively little modulation in task positive regions, they showed greater deactivation with more recalled details in medial parietal cortex, a part of the task negative network, compared to young subjects (Fig. 2c). These findings indicate that when young people showed more activation than old for recall of the gist, the extent of activation contributed to forming richer and more detailed memories, while older subjects show these effects for deactivation.

A similar comparison was made between old PIB+ and PIB– subjects to examine the effect of amyloid on parametric increases in encoding activity. Older PIB+ subjects show stronger parametric effects than PIB– subjects in parietal and occipital cortex, particularly in the right hemisphere (Fig. 2d, Supplementary Table 6). PIB+ individuals showed greater increases in brain activation across superior and lateral parietal as well as medial and lateral occipital cortex related to the number of details encoded (Fig. 2e). Old PIB– subjects again showed a minimal parametric response in task positive regions, but greater linear decreases in task negative regions, including right angular gyrus and medial parietal cortex, as more details were recalled (Fig. 2f). The PIB+ subjects showed relatively little linear decrease in these areas. The results were similar when PIB Index was treated as a continuous variable rather than dichotomizing subjects into groups. That is, there were greater linear increases in task positive lateral occipital cortex at higher levels of PIB Index and reduced linear decreases in the task negative medial parietal cortex (Supplementary Fig. 4). We additionally found that, among PIB+ individuals, the parametric increases apparent in task positive regions were attenuated at the highest levels of amyloid accumulation (see Supplementary Fig. 5). It should be noted however that even these high PIB subjects tended to show greater parametric increases than the PIB– group as a whole.

The parametric relationship between neural activity and memory richness is evidence that increased neural activity in those with brain Aβ is a beneficial process that reflects neural plasticity and serves a compensatory function. We also confirmed previous reports of reduced modulation of deactivation in PIB+ individuals[6], consistent with the idea that increased activation may also be related to this loss of deactivation in task negative regions. Deposition of Aβ interferes with a variety of neural functions including long-term potentiation[12] and induces aberrant local circuit properties[13]. Aβ is also associated with reduced task-positive network connectivity[14], and abnormal task-negative and task-positive network function could result in inefficient neural processes necessitating greater neural

activity. Similar mechanisms have been proposed due to age-related changes[15,16], and could reflect the mechanism whereby older people with brain Aβ deposition are able to remain cognitively normal while those unable to recruit these resources decline.

Consistent with previous findings that hippocampal hyperactivity among MCI subjects appears to be non-specific[17], we did not find parametric increases of activity in the medial temporal lobe related to detailed memory formation. Thus, it is possible that previous reports of heightened hippocampal activity in individuals with amyloid deposition or more advanced MCI could reflect a different underlying mechanism[7] or a disease progression in which initial compensatory mechanisms begin to fail[18]. Indeed, we did find reduced parametric increases in subjects with the highest levels of amyloid deposition (Supplementary Fig. 5).

The long-term consequences of brain Aβ deposition are still incompletely understood. It remains possible that individuals with brain Aβ and normal cognitive function are destined for eventual cognitive decline as neural inefficiency eventually increases to the point where compensation is no longer effective. In fact, this neural inefficiency itself may ultimately result in the deposition of increased Aβ, which is released through neural activity at the synapse[19,20]. The reduced parametric relationship between activation and performance in subjects with the highest levels of deposition (Supplementary Fig. 5) suggests that, at the very least, these regions make declining contributions to memory formation with continued amyloid accumulation. Whether and how individuals with brain Aβ can remain cognitively healthy for long periods of time is a question that will require longitudinal observation of behavior and neural function.

Online Methods

Participants

Seventy-four healthy elderly subjects underwent [^{11}C]PIB-PET and fMRI scanning and 31 young subjects underwent fMRI scanning for this study (see Table 1 for subject characteristics). MRI scans were acquired within an average of 72 days of the PET scan (SD=181.6 days, range=0–1,263 days, median=25 days). The subject with a delay of 1,263 days was strongly PIB+, and thus would be expected to remain in this group over time. All elderly subjects underwent a detailed battery of neuropsychological tests described previously[21]. All subjects were a subgroup of individuals who were recruited from the community via newspaper advertisements, talks at senior centers, or word of mouth; young subjects were recruited from online subject registries. All subjects underwent a medical interview and a detailed battery of neuropsychological tests. In order to be eligible for the study, older subjects were required to be 65 years or older, live independently in the community without neurological or psychiatric illness, and have no major medical illness or medication that influenced cognition. All subjects' neuropsychological performance was within age-adjusted normal range (i.e., within 1.5 SD from the mean scores). Although longitudinal follow-up data on these older subjects are not available yet, none of subjects reported cognitive symptoms at the time of participation. Apolipoprotein E (ApoE) ε4 carrier status was determined for older subjects using previously published methods[22]. All subjects provided informed consent in accordance with the Institutional Review Boards of

the University of California, Berkeley, and the Lawrence Berkeley National Laboratory (LBNL). Twenty-five elderly and 9 young subjects were excluded due to poor performance (<45% hit rate on the gist task; N = 8), problems with data collection (behavioral, MRI or PET; N = 11), or excessive motion (N = 15), resulting in a total number of 49 cognitively normal old and 22 young subjects for data analysis. Eight elderly and one young subject included in the present study participated in an experiment of episodic memory encoding previously published from our laboratory[7]. There were no significant differences between the groups in the number of subjects excluded for any of the above reasons.

Behavioral Procedure

The memory task used here was adapted from Qin et al.[9]. Subjects completed a scanned encoding session during which 150 pictures of scenes were presented over 3 functional runs (Supplementary Fig. 1). Images were presented on a black background for 6.6s, during which subjects responded whether there were people or no people in the scene with a button press using a 4-button response box using either thumb (response mappings were counterbalanced across subjects). A white fixation cross then appeared for 1–4 TRs (mean ITI = 4s) before moving on to the next trial.

Following a 15 minute delay, the subsequent memory test phase took place outside of the scanner on a desktop computer. This session was composed of two tasks that we refer to as the gist and details tasks, each split into 3 blocks. During the gist task, which lasted approximately 30 minutes, subjects were presented a total of 150 written descriptions of studied scenes, intermixed with 150 descriptions of unstudied scenes. Subjects were instructed to decide whether each description was associated with an old (presented during encoding) or new (not presented during study) scene as well as their confidence in the response (high or low). During the details task, which lasted approximately 90 minutes, only memory for the 150 scenes presented at encoding was assessed. For each encoded item, subjects were first presented the associated gist description, followed by a set of 6 details related to the scene. Subjects were instructed to respond whether each detail was true or false. The number of true details varied randomly from 2–4 across trials. Responses were made with a key press and subjects were given a maximum of 10s to respond for each item. The order of item presentation during the memory tests was varied randomly for each subject.

PIB-PET Acquisition

[^{11}C]PIB (PIB) was synthesized at the LBNL Biomedical Isotope Facility using a published protocol and described in detail previously[23]. PIB-PET imaging was performed at LBNL using an ECAT EXACT HR or BIOGRAPH Truepoint 6 scanner (Siemens Medical Systems, Erlangen, Germany) in 3D acquisition mode. Approximately 15 mCi of PIB was injected into an antecubital vein. Immediately upon injection, dynamic acquisition frames were obtained as follows: 4 × 15 sec, 8 × 30 sec, 9 × 60 sec, 2 × 180sec, 10 × 300sec, and 2 × 600 sec (90 min total). Ten minute transmission scans for attenuation correction or x-ray CT were obtained for each PIB scan. PET data were reconstructed using an ordered subset expectation maximization algorithm with weighted attenuation. Images were smoothed with a 4 mm Gaussian kernel with scatter correction.

MRI Acquisition

Subjects were scanned in a 1.5T Magnetom Avanto (Siemens Medical Systems, Erlangen, Germany) scanner at LBNL. Each of the 3 functional runs were acquired with a T2*-weighted echo-planar imaging (EPI) sequence [TR=2200ms; TE=50; flip angle=90°; matrix=64×64; FOV=220mm; voxel size=3.44×3.44×3.4mm, duration=9 minutes]. 28 axial slices oriented to the AC-PC were acquired in an interleaved order giving whole brain coverage. Two-hundred and forty-six volumes were collected during each of the functional runs. The first 5 volumes of each run were discarded to allow for magnetization preparation. A high resolution magnetization-prepared rapid-acquisition gradient echo (MPRAGE) [TR=2110ms; TE=3.58 ms; matrix=256×256; FOV=256; sagittal plane; voxel size=1×1×1mm; 160 slices] and an in-plane turbo inversion recovery image [TR=2000ms; TE=11; matrix=256×256; FOV=220; voxel size=0.9×0.9×3.4mm, 28 slices] were collected for registration purposes.

PIB-PET Processing

All PIB-PET data was pre-processed using SPM8 software[24]. The first 5 frames were summed, and all frames including the summed image were realigned to the middle frame (17th frame). The subject's structural data was coregistered to their PIB-PET data using the mean image of frames corresponding to the first 20 minutes of acquisition as a target. PIB distribution volume ratio (DVR) images were created using Logan graphical analysis with frames corresponding to 35–90 min post-injection and a gray matter (GM) cerebellum reference region defined using FreeSurfer v5.1 software[25–27]. Mean DVR values from frontal, parietal, temporal, and cingulate cortices were computed to serve as a global PIB index for all older subjects.

Elderly subjects were dichotomized into PIB– and PIB+ groups based on a cut-off defined from a group of 18 young subjects who received PIB-PET scans and showed no signs of PIB uptake. Eleven of these subjects were scanned on the ECAT HR and 7 on the Biograph; the mean and standard deviations for the global PIB DVRs were almost identical (Ecat: mean = 1.014, SD = 0.023; Biograph: mean = 0.993, SD = 0.036). These subjects were presumed to be Aβ-free and provide a baseline level of absent PIB binding. Using a method previously reported, the PIB positivity cut-off was taken as 2 standard deviations (SD) above the mean PIB Index value of these young subjects (mean = 1.01, SD = 0.03), resulting in a value of 1.07[7]. Experimenters were blinded to subjects' PIB status during data collection.

fMRI Processing

fMRI data were preprocessed and analyzed with the FSL toolbox v5.0[28]. Motion correction was performed with MCFLIRT, aligning all images to the middle slice with rigid body transformation. Slice timing correction was performed using (Hanning windowed) sinc interpolation to shift each slice in the volume in reference to the middle of the TR period. BET (brain extraction tool) was then used to create a mask of the brain from the first volume of each time series and used to separate brain from surrounding skull and tissue in each volume. All images were spatially smoothed with a 6mm FWHM Gaussian kernel to reduce noise. Highpass temporal filtering was performed with a 100s cut-off using the local Gaussian-weighted fit of a running line to remove low frequency artifacts. Subject data were

registered to standard space in a three-step process using FNIRT (FMRIB's Non-Linear Image Registration Tool). First, EPIs were linearly registered to each subject's skull-stripped in-plane anatomical image. Second, the in-plane anatomical image was linearly registered to the skull-stripped high resolution T1-weighted image. Third, subject's T1-weighted images were non-linearly registered to standard space (FSL's MNI152 template). The three registrations were then combined to take the subject's EPI images and run-level statistical maps into standard space in one transformation. GM partial volume maps were generated using FSL's FAST tool in order to be included as voxelwise regressors controlling for atrophy. The smoothing of these maps was matched to that of the functional images after registration to standard space.

fMRI Analysis

Individual runs from the encoding session were modeled in subject space using FSL's FEAT v6.0 tool, and resulting statistical maps were registered to standard space for higher level analysis. Separate models were generated for the gist and details tasks. For the gist model, trials were classified as hits or misses. Hits and misses were collapsed across confidence level in order to ensure a sufficient number of events per condition. In the details model, hits and misses were further categorized by the number of details correctly recalled (e.g., Hit_1, Miss_1, Hit_2, Miss_2, etc.). Regressors of interest were obtained by convolving stimulus onset times with FSL's double gamma hemodynamic response function and their temporal derivative. Motion parameters and outlier volumes (defined as excessive motion or intensity) were included as additional confound variables and temporal autocorrelation was removed through pre-whitening. A contrast of hits versus baseline was generated for the gist task to measure relative activations and deactivations for encoded items. A linear contrast was formed in the details model to assess activity parametrically modulated by the number of details encoded. Only trials classified as hits during the gist task were included and detail levels 0–1 and 5–6 were combined to increase the number of events within these conditions. This resulted in linear contrast of [Hit_5+6 > Hit_4 > Hit_3 > Hit_2 > Hit_0+1].

A second level analysis combined these contrasts from the 3 runs for each subject using a one-sample t-test, treating runs as fixed effects. Third-level group statistics maps were created using the Robust Biological Parametric Mapping (rBPM) toolbox [29,30], treating subjects as a random factor. rBPM allows for the inclusion of voxelwise regressors and implements a robust regression model (using the bisquare weight function) to reduce sensitivity to outliers. Performance and GM partial volume maps were included as nuisance regressors, and the average was taken across all three groups. The age effect was assessed by comparing the young and old PIB– groups including GM partial maps and performance (hit rate) as nuisance regressors. The PIB effect was assessed by comparing old PIB+ and old PIB– groups including GM partial volume maps, performance (hit rate) and age as nuisance regressors. Performance was included to account for individual differences on the memory task and to account for varying number of hit trials included in contrasts across subjects. The whole brain family-wise error was cluster corrected to $p<0.05$ (two-sided) using a cluster forming threshold of $p<0.05$. Thresholded statistical maps were projected on to inflated atlases for display purposes using Caret v5.64 software[31]. The group comparisons do not distinguish between increased activation and reduced deactivation. Therefore, we examined

the relative directionality of significant voxels by masking them with task-positive and task-negative network maps derived from comparing hits to baseline averaged across all groups (i.e., Fig. 1a). These masked results as well as plots displaying average activity of significant clusters falling within each masked region are presented for visualization purposes.

A supplementary methods checklist is available.

Supplementary Material

Refer to Web version on PubMed Central for supplementary material.

Acknowledgments

The authors would like to thank Shaozheng Qin for task stimuli and Willem Huijbers for useful discussion. This work was supported by NIH grant AG034570.

References

1. Jack CR, et al. Tracking pathophysiological processes in Alzheimer's disease: an updated hypothetical model of dynamic biomarkers. Lancet Neurol. 2013; 12:207–216. [PubMed: 23332364]
2. Bennett DA, et al. Neuropathology of older persons without cognitive impairment from two community-based studies. Neurology. 2006; 66:1837–1844. [PubMed: 16801647]
3. Morris JC, et al. APOE predicts amyloid-beta but not tau Alzheimer pathology in cognitively normal aging. Ann Neurol. 2010; 67:122–131. [PubMed: 20186853]
4. Aizenstein HJ, et al. Frequent amyloid deposition without significant cognitive impairment among the elderly. Arch Neurol. 2008; 65:1509. [PubMed: 19001171]
5. Sperling RA, et al. Toward defining the preclinical stages of Alzheimer's disease: Recommendations from the National Institute on Aging-Alzheimer's Association workgroups on diagnostic guidelines for Alzheimer's disease. Alzheimers Dement. 2011; 7:280–292. [PubMed: 21514248]
6. Sperling RA, et al. Amyloid Deposition Is Associated with Impaired Default Network Function in Older Persons without Dementia. Neuron. 2009; 63:178–188. [PubMed: 19640477]
7. Mormino EC, et al. Aβ Deposition in Aging Is Associated with Increases in Brain Activation During Successful Memory Encoding. Cereb Cortex. 201110.1093/cercor/bhr255
8. Dickerson BC, et al. Medial temporal lobe function and structure in mild cognitive impairment. Ann Neurol. 2004; 56:27–35. [PubMed: 15236399]
9. Qin S, van Marle HJF, Hermans EJ, Fernández G. Subjective Sense of Memory Strength and the Objective Amount of Information Accurately Remembered Are Related to Distinct Neural Correlates at Encoding. J Neurosci. 2011; 31:8920–8927. [PubMed: 21677175]
10. Naghavi HR, Nyberg L. Common fronto-parietal activity in attention, memory, and consciousness: shared demands on integration? Conscious Cogn. 2005; 14:390–425. [PubMed: 15950889]
11. Raichle ME, et al. A default mode of brain function. Proc Natl Acad Sci. 2001; 98:676–682. [PubMed: 11209064]
12. Walsh DM, et al. Naturally secreted oligomers of amyloid β protein potently inhibit hippocampal long-term potentiation in vivo. Nature. 2002; 416:535–539. [PubMed: 11932745]
13. Palop JJ, Mucke L. Amyloid-[beta]-induced neuronal dysfunction in Alzheimer's disease: from synapses toward neural networks. Nat Neurosci. 2010; 13:812–818. [PubMed: 20581818]
14. Oh H, Jagust WJ. Frontotemporal Network Connectivity during Memory Encoding Is Increased with Aging and Disrupted by Beta-Amyloid. J Neurosci. 2013; 33:18425–18437. [PubMed: 24259567]

15. Morcom AM, Li J, Rugg MD. Age Effects on the Neural Correlates of Episodic Retrieval: Increased Cortical Recruitment with Matched Performance. Cereb Cortex bhl155. 200710.1093/cercor/bhl155
16. Spreng RN, Wojtowicz M, Grady CL. Reliable differences in brain activity between young and old adults: A quantitative meta-analysis across multiple cognitive domains. Neurosci Biobehav Rev. 2010; 34:1178–1194. [PubMed: 20109489]
17. Zamboni G, et al. Resting Functional Connectivity Reveals Residual Functional Activity in Alzheimer's Disease. Biol Psychiatry. 2013; 74:375–383. [PubMed: 23726515]
18. O'Brien JL, et al. Longitudinal fMRI in elderly reveals loss of hippocampal activation with clinical decline. Neurology. 2010; 74:1969–1976. [PubMed: 20463288]
19. Cirrito JR, et al. Synaptic Activity Regulates Interstitial Fluid Amyloid-β Levels In Vivo. Neuron. 2005; 48:913–922. [PubMed: 16364896]
20. Jagust WJ, Mormino EC. Lifespan brain activity, β-amyloid, and Alzheimer's disease. Trends Cogn Sci. 2011; 15:520–526. [PubMed: 21983147]
21. Oh H, Habeck C, Madison C, Jagust W. Covarying alterations in Aβ deposition, glucose metabolism, and gray matter volume in cognitively normal elderly. Hum Brain Mapp. 2014; 35:297–308. [PubMed: 22965806]
22. Agosta F, et al. Apolipoprotein E ε4 is associated with disease-specific effects on brain atrophy in Alzheimer's disease and frontotemporal dementia. Proc Natl Acad Sci. 2009; 106:2018–2022. [PubMed: 19164761]
23. Rabinovici GD, et al. 11C-PIB PET imaging in Alzheimer disease and frontotemporal lobar degeneration. Neurology. 2007; 68:1205–1212. [PubMed: 17420404]
24. Friston, KJ.; Ashburner, JT.; Kiebel, SJ.; Nichols, TE.; Penny, WD. Statistical Parametric Mapping: The Analysis of Functional Brain Images: The Analysis of Functional Brain Images. Academic Press; 2011.
25. Logan J, et al. Distribution Volume Ratios Without Blood Sampling from Graphical Analysis of PET Data. J Cereb Blood Flow Metab. 1996; 16:834–840. [PubMed: 8784228]
26. Price JC, et al. Kinetic modeling of amyloid binding in humans using PET imaging and Pittsburgh Compound-B. J Cereb Blood Flow Metab. 2005; 25:1528–1547. [PubMed: 15944649]
27. Dale AM, Fischl B, Sereno MI. Cortical Surface-Based Analysis: I Segmentation and Surface Reconstruction. NeuroImage. 1999; 9:179–194. [PubMed: 9931268]
28. Smith SM, et al. Advances in functional and structural MR image analysis and implementation as FSL. Neuroimage. 2004; 23:208–219.
29. Casanova R, et al. Biological Parametric Mapping: A Statistical Toolbox for Multi-Modality Brain Image Analysis. NeuroImage. 2007; 34:137–143. [PubMed: 17070709]
30. Yang X, Beason-Held L, Resnick SM, Landman BA. Biological parametric mapping with robust and non-parametric statistics. NeuroImage. 2011; 57:423–430. [PubMed: 21569856]
31. Van Essen DC. A population-average, landmark-and surface-based (PALS) atlas of human cerebral cortex. NeuroImage. 2005; 28:635–662. [PubMed: 16172003]

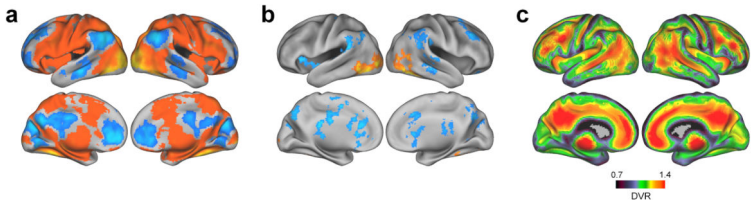

Fig. 1. Group imaging results

a.) Regions demonstrating encoding activation and deactivation related to successful gist memory (hits versus baseline) across all subjects. Warm colors indicate activation and cool colors indicate deactivation. b.) Regions demonstrating parametric encoding activation related to level of detail memory across all groups were defined by averaging the linear contrasts of gist hits classified by the number of correctly identified details. Warm colors indicate linear increases in brain activity with more details and cool colors indicate linear decreases. Results in panels a and b are thresholded at $p<0.05$, cluster corrected for multiple comparisons. c.) A map of PIB binding in individuals demonstrating Aβ deposition was defined by averaging the PET images of subjects whose PIB Index exceeded 1.07 (PIB+). Warm colors indicate higher Aβ deposition.

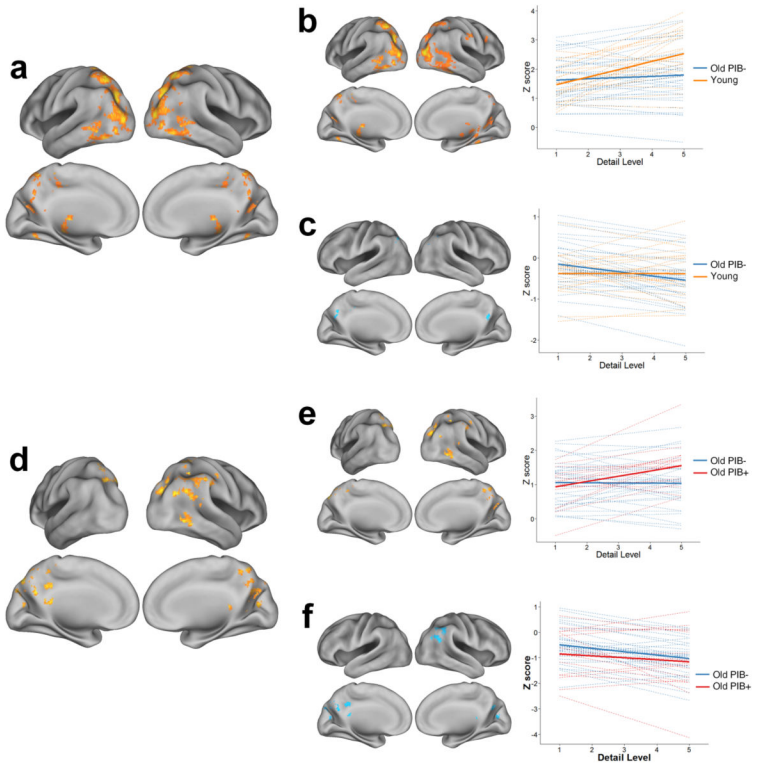

Fig. 2. Age and Aβ effects on parametric encoding activity for details

Linear contrasts of activity related to number of details correctly recalled were assessed for age and PIB effects. Only items correctly remembered on the gist task were included. To distinguish between relative increases and decreases from baseline activity, tests of age (panel a) and PIB (panel d) were masked by task positive and negative networks (defined by contrasting hits with baseline, averaged across all groups) shown in Fig. 1a. Plots displaying mean z-scores of significant clusters accompany masked results to better visualize underlying patterns of activity in the voxelwise analysis. Dashed lines represent subject-level linear regression lines and solid lines represent group estimates. a.) Greater linear increases in activity across detail level in young compared to old PIB– subjects (warm colors). b.) Task positive regions show differences due to greater linear increases in young than PIB– subjects (warm colors). c.) Task negative regions indicate greater linear decreases in PIB– subjects than young (cool colors). d.) Aβ effects revealed greater linear increases in old PIB+ compared to PIB– subjects (warm colors). e.) Task positive regions indicate greater detail-related activation in old PIB+ than PIB– subjects (warm colors). f.) Task negative regions show differences due to reduced detail-related deactivation in old PIB+ compared to PIB– subjects (cool colors). Results are thresholded at $p<0.05$, cluster corrected for multiple comparisons.

Table 1

Group characteristics

Standard deviations are listed in parentheses. All groups performed similarly on both gist and detail tasks.

	Old PIB+	Old PIB–	Young
N	16	33	22
Age	75.56 (4.68)	76.82 (5.32)	23.64 (2.04)
Gender	7M	13M	11M
Education	16.37 (2.28)	16.67 (1.71)	15.95 (1.25)
APOε4 carriers/noncarriers	6/8	5/28	NA
Gist Hit Rate	0.71 (0.11)	0.67 (0.11)	0.64 (0.13)
Gist Correct Rejection Rate	0.77 (0.15)	0.82 (0.09)	0.82 (0.12)
Gist *d*-prime	1.40 (0.40)	1.40 (0.32)	1.37 (0.40)
Detail Accuracy (per trial)	3.30 (0.19)	3.25 (0.19)	3.37 (0.25)
PIB Index	1.22 (0.15)	0.99 (0.05)	NA
MMSE	28.56 (1.37)	28.85 (1.37)	NA